Return to previous file: MCU12a.pdf

Figure 10 shows the resultant residual current plots for tides plus weak WCC conditions plus easterly storm waves (Figure 10a), tides plus average WCC conditions plus average waves (Figure l0b) and tides plus strong WCC conditions plus southerly storm waves (Figure 10 c).

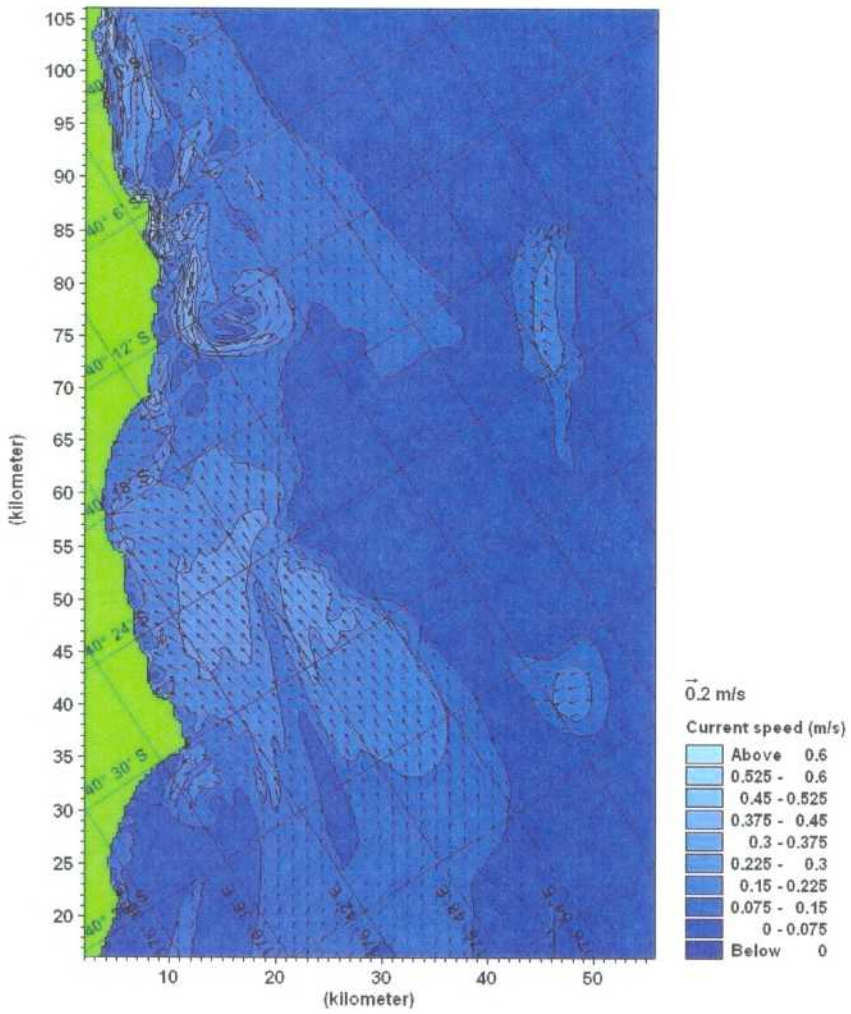

Figure 10a: Combined residual currents for weak WCC conditions with tides plus easterly storm wave conditions.

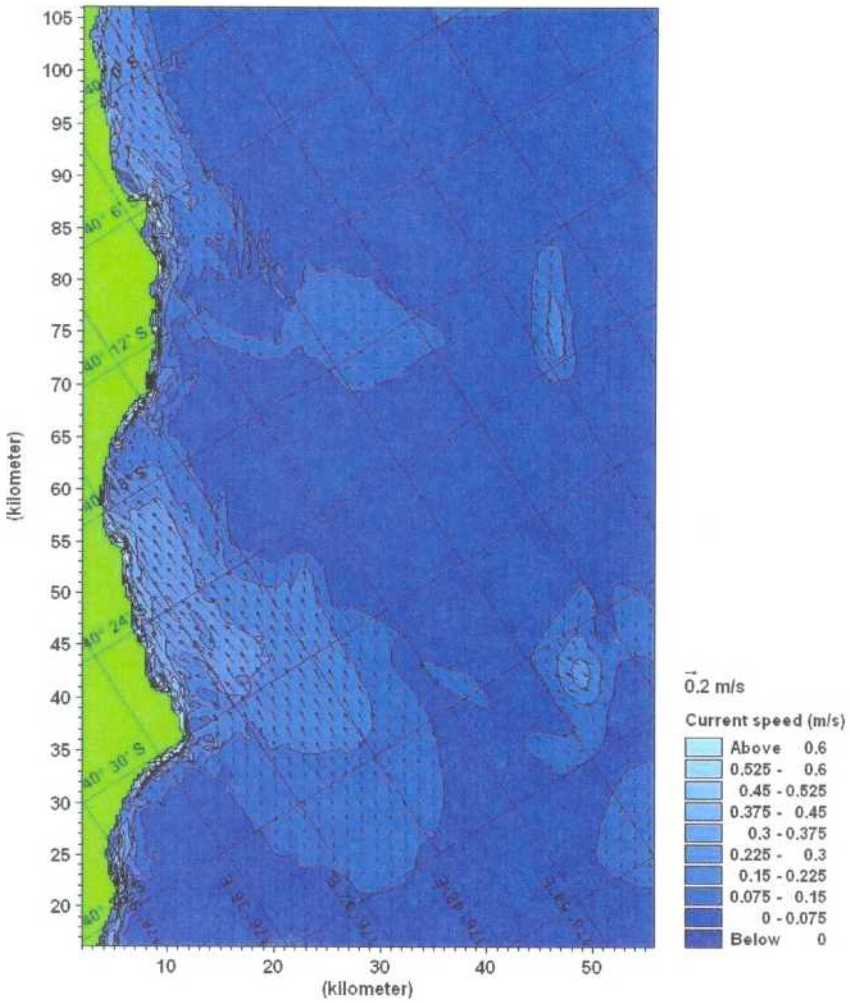

Figure l0b: Combined residual currents for average WCC conditions with tides plus average wave conditions.

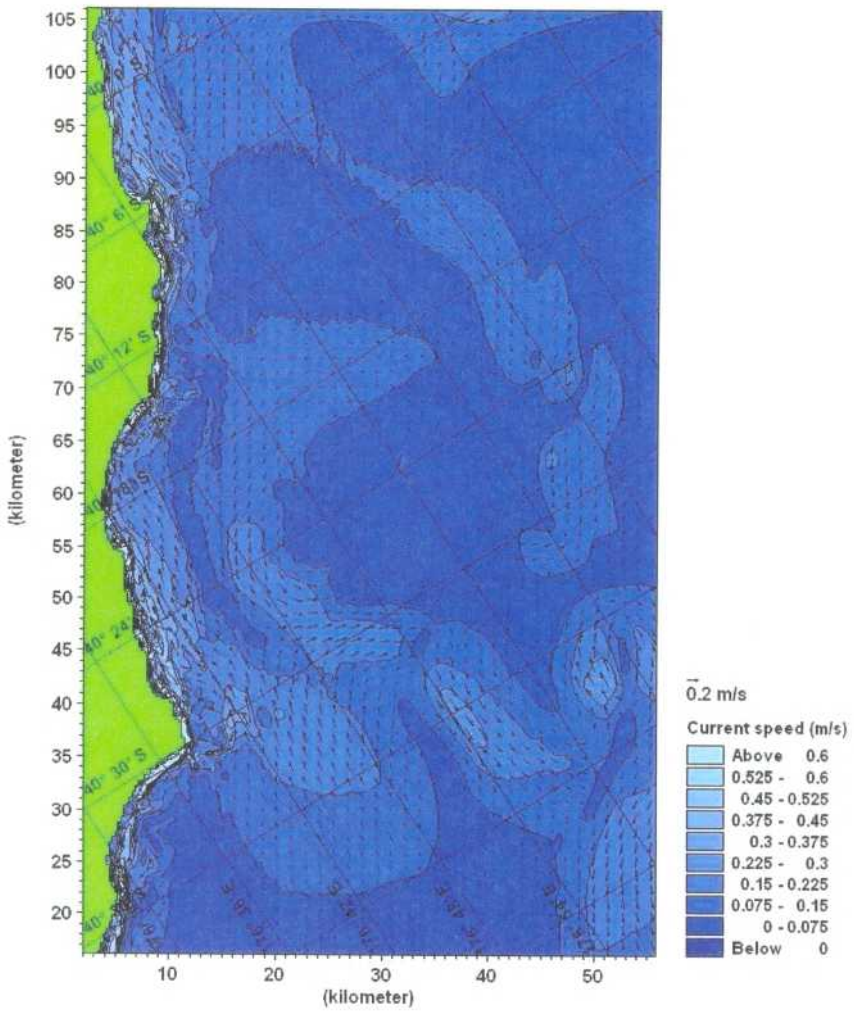

Figure 10c: Combined residual currents for strong WCC conditions with tides plus southerly storm wave conditions.

2.5 MIKE21 particle-analysis model

The particle-analysis model is based on the random walk technique where an ensemble of "particles" (larvae) is followed over time (i.e., lagrangian technique). The "particles" move due to the advective current (which was specified as logarithmic in the vertical) and turbulent fluctuations. The advective velocities are obtained from the hydrodynamic simulations, whereas the turbulent contributions are controlled by dispersion coefficients.

Larval releases were represented by the continuous release of "particles" at each spawning area. Each particle was treated as an isolated mass with the particles regarded as fully mixed over the water depth. Particle settling took place with a constant settling velocity, thereby reducing the total remaining mass in suspension. Using this approach larvae can either remain in the water column, settle on the sea bed or reach their maximum age and die. Results are given in terms of the percentage of total larvae that have settled.

The flow fields calculated using the hydrodynamic model and used for advection of particles in the particle-analysis model are calculated in a grid of a certain spatial resolution (270 m) and timestep (15 min). Physical flow processes, however, occur at different spatial and temporal scales with a continuous spectrum ranging from tiny molecular agitation to large-scale oceanic currents. It is simply too computationally expensive to calculate the tiny molecular processes across the spatial scales of the large domain, which means the model is simplified into grid cells much larger than the intermolecular spacing associated with molecular agitation processes. To take these effects into account, an artificial dispersion is applied that is a mathematical artefact arising from the spatial averaging rather than a physical process. This dispersion has the effect of transferring some of the mass of larvae away from the source which allows a more realistic dispersal of the larvae. Selecting correct dispersion coefficients is dependent on obtaining coefficients from a calibration process where simulated and measured concentration fields are compared. These data are seldom available and have not been collected for this study. Particle dispersion was set proportional to the current velocity, using the model default values of 1, 0.1 and 0.01 $m^2 s^{-1}$ respectively in the longitudinal, transverse and vertical directions. This longitudinal value is in about the middle of the expected range (0.27-6.75 $m^2 s^{-1}$ for the grid size and timestep used (DHI Water and Environment, MIKE21-PA manual, 2003).

2.6 Larval species and release points

As for the previous study (Stephens et al. 2004) five species of larvae were modelled with different fall velocities and larval durations. Four release sites were identified as follows:

- RI: Cape Tumagain (average depth = 1.6 below chart datum);
- R2: Porangahau River (average depth = 2.0 below chart datum);
- R3: Blackhead Point (average depth = 1.1 below chart datum);

- R4: Marine Reserve (average depth = 1.8 below chart datum).

For each of these locations, the particles simulating the larvae were released into three near-shore model cells (covering a 810 m length of coastline) and their movements were simulated for 0.5, 4, 10, 20 or 30 days. The fall velocity and larval duration periods for the five species is specified in Table 3. The mean number of larvae settled (as a percentage of the total number of larvae settled) at the end of each of the simulations was calculated. Plots of the predicted settled larvae are given in Appendix 1 - 4. The tables in Appendix 5 - 8 summarises the model output for each of the simulations.

Table 3: Details of larval duration and assumed fall velocity for the target species.

Common name	Species	Larval duration (days)	Fall velocity (m/s)
Bull kelp	*Durvillaea*	0.25-0.5	0.0036
Bubu	*Turbo smaragdus*	0.25-0.5	0.0001
Bubu, Cook's turban	*Cookia sulcata*	0.25-0.5	0.0001
Ngakihi, limpets	*Cellana* spp	2-10	0.0001
Black foot paua	*Haliotis iris*	3-11	0.0001
Kina	*Evechinus chloroticus*	20-30	0.0001

2.7 Predicted larval dispersal patterns

The plots contained in Appendices 1 - 4 show the predicted distribution of settling under the four different forcing conditions for the five species under consideration. The plots show settled larvae in each cell (each cell being an area of 72,900 m^2), given as a percentage of the total amount of settled larvae. Figure 11 gives an example of the plots presented in appendices 1 - 4. Near the source, a value of 1 (indicated by the orange colour on the side colour bar) is predicted. This indicates that near the source one-percent of the total number of larvae have settled in each cell after 10 days. Moving away from the source the number of settled larvae declines. Near Blackhead Point the number of larvae settling per cell is around 0.02 percent of the total number of settled larvae (the colour bar is plotted on a log scale so 0.02 (light blue) sits mid way between 0.1 and 0.01). Between the source and Blackhead Point it is predicted

that 0.2 percent (indicated by the yellow shading) of the total number of settled larvae settle in each cell. For this simulation the larvae are predicted to settle up to 6480 m up the coast and up to 2430 m offshore.

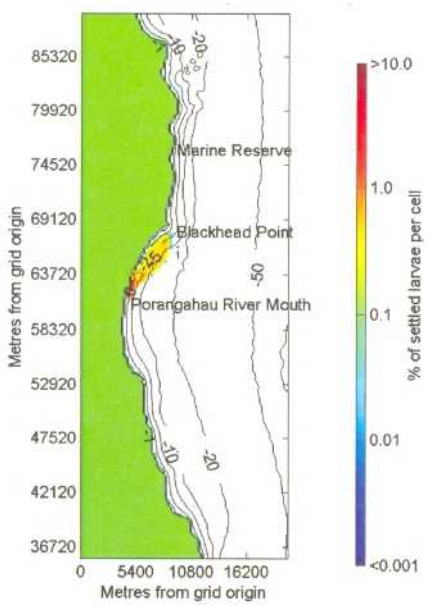

Figure 11: Example plot of the larval settling pattern for a 10-day simulation of bubu released near the mouth of the Porangahau River under the influence of a strong WCC, southerly storm waves and tides.

Kelp have the shortest larval duration (0.25 - 0.50 days) and highest fall velocity (0.0038 m/s). Plots for this species are given for a 12-hour model simulation.

Bubu, limpet and paua have the same fall velocity and varying larval duration (Table 3). Plots after 4 days and 10 days are presented for generic larvae of this fall size. The 4 days plots can be viewed as maximum dispersal predictions for bubu and minimum for limpet and paua. The 10-day plots show the maximum predicted dispersal patterns for limpet and paua.

As kina have the longest larval duration of all the species (20-30 days) plots are presented for 20 and 30-day model simulations.

2.7.1 Release point 1 (Cape Turnagain)

Figures 12 a - d show the predicted residual currents for the four conditions modelled in the vicinity of this release point. Under tides only a residual flow to the south exists at the headland. Just south of the headland a clockwise residual eddy is formed which creates a pathway for the transport of larvae offshore. On the southern extent of the eddy the residual flow pattern moves inshore. Under tides, weak WCC conditions and easterly storm wave conditions the residual currents are parallel up the coast to the north of the headland and down coast (and inshore) to the south of the headland. Under tides, average WCC and wave conditions the residual currents are parallel up the coast to the north of the headland. Near the coast wave radiation stress enhances the up coast residual current. To the south of the headland the residual offshore run parallel to the coast. Close to the coast wave radiation stress sets up strong down coast residual currents. A residual eddy current forms in the deeper water directly offshore of the headland. Under tides, strong WCC and southerly storm wave conditions the residual currents in the near shore zone become dominated by the effects of the wave radiation stress. Strong residuals either side of the headland are formed setting up a pathway of transport away from the headland both up and down the coast. Residual currents either side of the headland generally run parallel to the shoreline. Directly offshore of the headland complex patterns of residual currents are predicted.

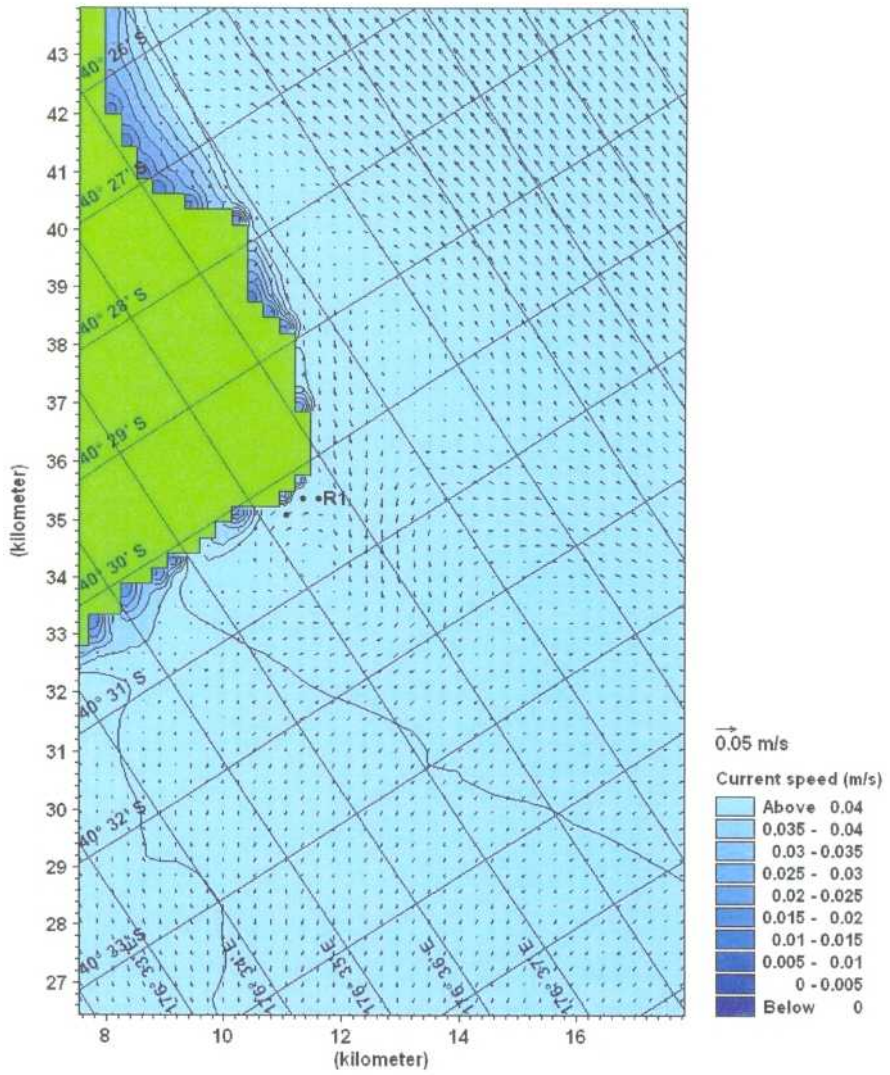

Figure 12a: Predicted residual tidal currents in the vicinity of Cape Turnagain.

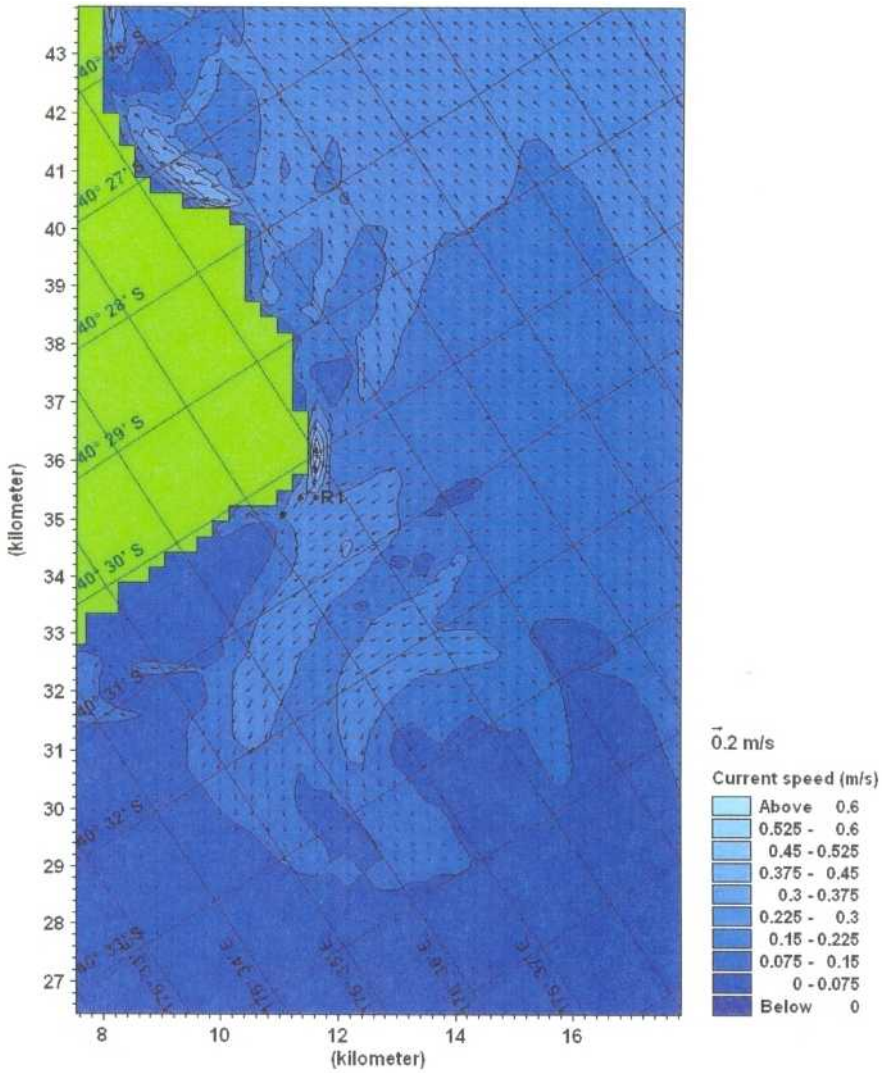

Figure 12b: Predicted residual currents in the vicinity of Cape Turnagain under conditions of a weak Wairarapa Coastal Current, easterly storm wave conditions and tides.

Continue to next file: MCU12c.pdf